113 (1977).
(26) F. C. Goodrich, *Proc. Int., Congr. Surface Activity, 2nd, 1957*, **I**, 85 (1957).
(27) J. T. Davies and E. K. Rideal, "Interfacial Phenomena", Academic Press, New York, N.Y., 1961, p 236.
(28) P. J. Giordano, C. R. Bock, M. S. Wrighton, L. V. Interrante, and R. F. X. Williams, *J. Am. Chem. Soc.*, **99**, 3187 (1977).
(29) See ref 13, p 196.
(30) A. Harriman, *J. Chem. Soc., Chem. Commun.*, 777 (1977).
(31) M. S. Henry, *J. Am. Chem. Soc.*, **99**, 6138 (1977).
(32) Both our work and that of Harriman[30] give this value.
(33) L. Holland, "The Properties of Glass Surfaces", Wiley, New York, N.Y., 1964, Chapter 3.
(34) R. H. Doremus, "Glass Science", Wiley-Interscience, New York, N.Y., 1973, Chapters 12 and 14.
(35) H. Sobotka, M. Demeny, and J. D. Chanley, *J. Colloid Sci.*, **13**, 565 (1958).
(36) G. L. Gaines, Jr., *J. Colloid Interface Sci.*, **59**, 438 (1977).
(37) We received several micrograms of the solid, labeled "W-1 1975", in Nov 1976 and in the form of five precoated monolayers on cadmium arachidate–glass slides in June 1976. This material will be called the "original preparation" in the text and is labeled compound **5a** in ref 8.
(38) Unless a compound refers to one of our synthesis, the following formula shorthand will be employed: Ru(COOR)₂ for {(bpy)₂Ruᴵᴵ[bpy(COOR)₂]}²⁺ where R = C₁₈ (C₁₈H₃₇), C₁₆ (C₁₆H₃₃), Et (C₂H₅), or H as noted.
(39) Roughly estimated from the uncorrected emission spectra of our **Ia** (their **5d**) and the original preparation (**5a**) shown without a blank spectrum in Figure 3 of ref 8.
(40) R. L. Airey and F. S. Dainton, *Proc. R. Soc. (London), Ser. A*, **291**, 340, 478 (1966).

Hydrogen Bonding of Water to Gas-Phase Ions.
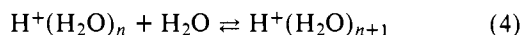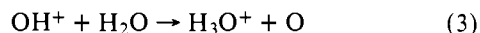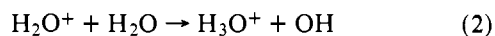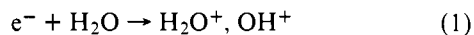# Structural and Stereochemical Effects in Protonated Phenols

D. P. Martinsen and S. E. Buttrill, Jr. *[1]

Contribution from the Department of Chemistry, University of Minnesota, Minneapolis, Minnesota 55455. Received September 12, 1977
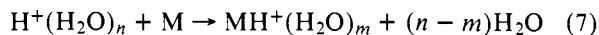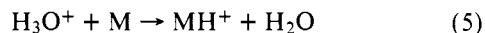
Abstract: The water chemical ionization mass spectra of substituted phenols M contain, in addition to the expected MH^+ ions, hydrogen-bonded clusters of the protonated phenol with water, $MH^+\cdot(H_2O)_n$ ($n = 1-3$). The relative intensities of these ions obtained at 120 °C and 0.3 Torr H_2O in a conventional ion source show significant differences which make it possible in most cases to distinguish ortho, meta, and para isomers. Using a new pulsed high-pressure source, equilibrium constants and ΔG at 450 K were measured for the reaction $MH^+ + H_2O \rightleftharpoons MH^+\cdot H_2O$ for 17 phenols. The excellent correlation between ΔG^{450} and the ratio of $MH^+\cdot H_2O$ to MH^+ in the conventional water CI spectra indicates that equilibrium, rather than kinetic effects, governs the relative intensities of these ions under CI conditions. Gas-phase hydrogen bond strengths are a sensitive new probe of the structure and intramolecular interactions of protonated molecules.

Introduction

In chemical ionization mass spectrometry,[2] the initial ionization, usually induced by high-energy electrons, occurs in a reagent gas present at pressures of 0.1–10 Torr in the mass spectrometer ion source. Although methane and isobutane are the most common reagent gases, we have used water extensively for the last few years.[3-7] The most important processes leading to the formation of the stable reagent ions in water[8] are summarized in the reactions

$$e^- + H_2O \rightarrow H_2O^+, OH^+ \tag{1}$$

$$H_2O^+ + H_2O \rightarrow H_3O^+ + OH \tag{2}$$

$$OH^+ + H_2O \rightarrow H_3O^+ + O \tag{3}$$

$$H^+(H_2O)_n + H_2O \rightleftharpoons H^+(H_2O)_{n+1} \tag{4}$$

The reactions of the hydronium ion and its hydrates with the sample molecules produce ions characteristic of the sample,

$$H_3O^+ + M \rightarrow MH^+ + H_2O \tag{5}$$

$$H^+(H_2O)_n + M \rightarrow MH^+ + nH_2O \tag{6}$$

$$H^+(H_2O)_n + M \rightarrow MH^+(H_2O)_m + (n - m)H_2O \tag{7}$$

In addition to these bimolecular processes (eq 5–7), the protonated sample may also form a hydrogen-bonded cluster with one or more water molecules through termolecular reactions.

$$MH^+ + 2H_2O \rightleftharpoons MH^+(H_2O) + H_2O \tag{8}$$

$$MH^+(H_2O)_n + 2H_2O \rightleftharpoons MH^+(H_2O)_{n+1} + H_2O \tag{9}$$
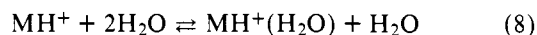
These last reactions are readily reversible and under appropriate conditions can lead to the establishment of thermo-chemical equilibrium among all or some of the ionic species present in the mass spectrometer ion source.[8,9]

One of our first observations regarding water CI spectra was that the relative intensities of the MH^+ and the $MH^+(H_2O)_n$ ions seemed to depend very much on the functional group protonated. When instrumental parameters, such as source temperature and pressure, are carefully controlled, these peaks provide analytically useful information on the structure and stereochemistry of the sample.[6] In order to study the origins of these useful and interesting effects, we have constructed a pulsed high-pressure ion source which enables us to monitor the time dependence of the ion concentrations and obtain both kinetic and thermochemical information about the formation of the hydrogen-bonded cluster ions. This paper reports our results from both conventional and pulsed high-pressure water chemical ionization mass spectrometry for some substituted phenols.

Experimental Section

The modifications to our Du Pont 21-490B mass spectrometer for conventional chemical ionization work have been described in previous publications.[3,5,7]

The new pulsed high-pressure source is shown in Figure 1. All parts are stainless steel except for the insulator ring, which is made of Macor machinable glass ceramic.[10] The shapes of the source block and source mounting plate are such that the insulator ring is shielded from the ions, electrons, and reactive species generated within the ion source. A potential difference of up to 12 V may be applied between the source block and mounting plate if necessary to extract the ions. For these experiments, this voltage was kept below 0.5 V.

Because of their critical importance in determining equilibrium thermodynamic properties of ions, special provisions were made for accurately measuring the temperature and pressure in the source. The source block is equipped with two heater wells extending the full width
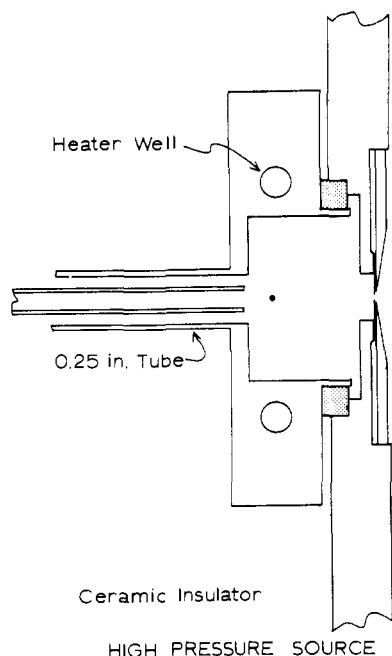
Figure 1. Cross section of the high-pressure ion source. See text. The solid dot shows the position of the electron beam.
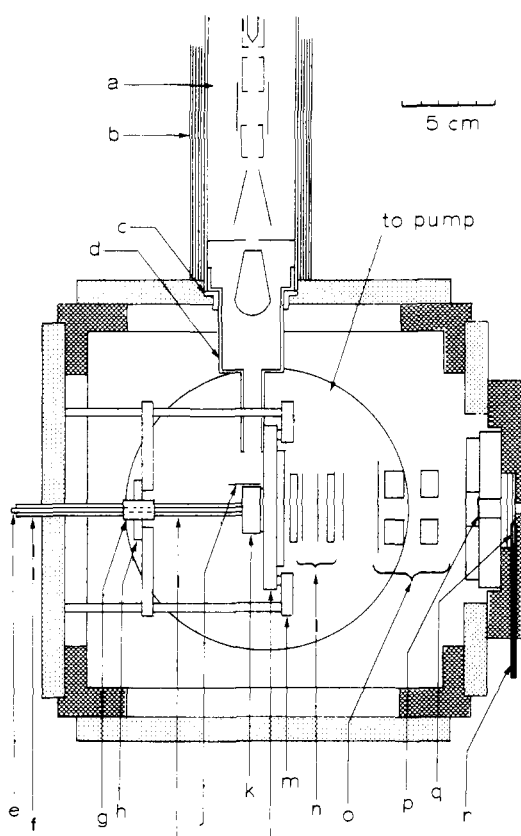

Figure 2. Cross-sectional view of the source housing showing the locations of the source, electon gun, and ion lenses: (a) electron gun assembly, (b) mu metal shield surrounding the gun outside the vacuum system, (c) Teflon washer and insulator, (d) magnetic shielding inside the vacuum system, (e) 3-mm glass tube for measuring source pressure, (f) 6-mm glass tube for gas inlet, (g) Swagelok bulkhead connector, (h) ceramic insulator, (i) 6-mm stainless steel tube for gas inlet, (j) fluorescent screen to aid in adjusting the electron beam, (k) ion source, (l) source mounting plate, (m) source support ring, (n) einzel lens system, (o) quadrupole lens system, (p) object slit, (q) Teflon gate valve, (r) 3-mm stainless steel rod used to open and close gate valve separating source and analyzer vacuum systems. The gate valve and drive rod are shown rotated 90° from their true position to clarify the drawing.
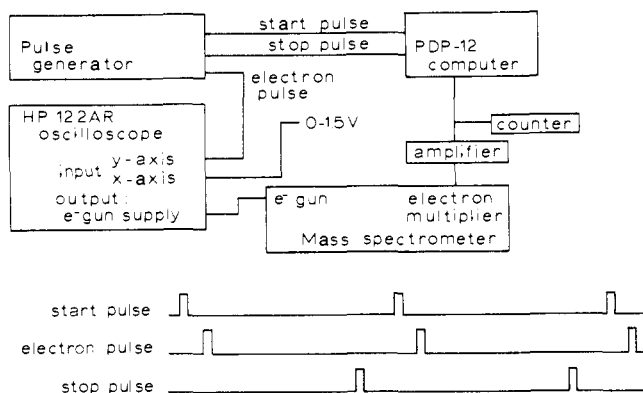

Figure 3. Diagram of the data collection system, electron beam pulsing system, and the pulse timing sequence. See text.

of the block (Figure 1). In addition, there are separate heaters (not shown) in the mounting plate, and the temperatures of both parts are monitored with separate thermocouples. The source is connected directly to the MKS Baratron capacitance manometer through a length of 3-mm glass tubing extending almost into the ionization region. The reagent gas flows through the annular space between this tube and the 6-mm stainless steel tube (Figure 1). There is no gas flow at all through the 3-mm tubing; thus there is no pressure difference between the ion source and the capacitance manometer sensor.

Figure 2 is a cross-sectional view of the new source housing showing the relative positions of the electron gun, source, ion lenses, and other major components. The 3500-V electron beam is produced and directed by a modified electron gun assembly from a Sylvania 5QP7 cathode ray tube. The cathode of the electron gun was replaced with a rhenium filament (0.025 × 0.75 mm ribbon). Except for the filament current, all lens voltages and control signals for the electron gun are supplied by a Hewlett-Packard 122 AR oscilloscope, which normally uses a 5QP7 CRT. The 0.5-μA electron beam enters the source through a 0.25-mm hole located 13 mm behind the 0.25-mm ion exit hole. Using these apertures, a pressure of 3 Torr could be maintained in the source while the pressure in the source housing was 5×10^{-5} Torr or less. Ions leaving the source enter an extraction region where a small (0–6 V/cm) field guides them into a simple two-element acceleration system.[11] The ions are then focused into a parallel circular beam by an einzel lens[12] and transformed into a ribbon-shaped beam by a set of dual electrostatic quadrupole lenses.[13]

The pulse sequence and data collection system for the equilibrium constant measurements are shown in Figure 3. The PDP 12/30 computer system is programmed to operate as a multichannel analyzer for these experiments with a time resolution of either 2.5 or 10 μs per channel. A start pulse from the pulse generator causes the computer to begin the data collection sequence. After a variable delay to compensate for the mass-dependent flight times of ions through the mass spectrometer, the electron beam pulse is sent to the y-axis input of the HP 122 AP oscilloscope chassis. This causes the electron beam to be deflected into the source for the duration (usually 10 μs) of the pulse. The stop pulse causes the computer to leave the data collection mode, add the data just accumulated into memory, and prepare for the next start pulse. A typical run in which ions are counted for 5 ms following the electron beam pulse for 100 000 cycles of the entire sequence takes about 10 min.

The raw data obtained during a measurement of the equilibrium constant for reaction 8 with M = o-chlorophenol is shown in Figure 4. Although the data were obtained using 10 μs per channel, they are plotted as counts per 50 μs for clarity. When the ion counts observed for a particular ionic species and 50 μs time window are normalized[14] to the total ion count during that time window, the results are curves such as those in Figure 5 of percent total ionization in the source for each species as a function of time following the pulse of ionizing electrons. After about 1 ms, all of the ionic species have come into equilibrium and thus have constant relative concentrations within the ion source. The equilibrium constant for reaction 8 is readily calculated from the ratio of $MH^+ \cdot (H_2O)$ to MH^+ and the measured pressure of water in the source. It is also possible to calculate a value of the equilibrium constant for the (3,4) equilibrium in pure water (reaction 4). Since the thermochemical parameters for these reactions are known[2,14,15] the accuracy of the latter equilibrium constant pro-
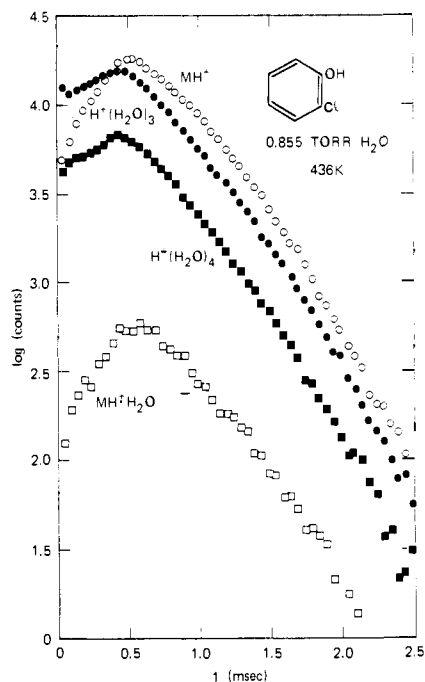
Figure 4. Plot of the logarithm of the ion counts per 50 μs channel vs. time for *o*-chlorophenol in H_2O at 0.855 Torr and 436 K: O, MH^+; □, $MH^+\cdot H_2O$; ●, $H^+(H_2O)_3$; ■, $H^+(H_2O)_4$.
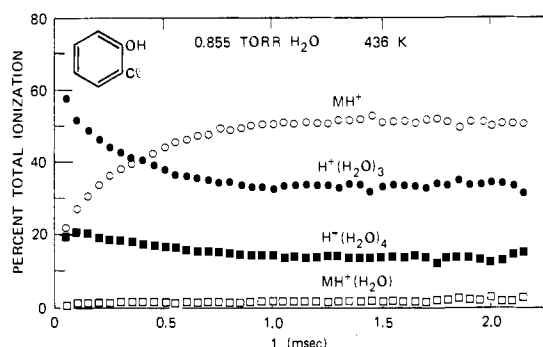
Figure 5. Data of Figure 4 plotted as percent of total ionization vs. time.

Figure 6. van't Hoff plot of log K for the indicated water equilibria vs. $1000/T$. The solid lines are calculated from the values of ΔH and ΔS for these equilibria given in ref 14 and 15.

Table I. Water Chemical Ionization Spectra of Substituted Phenols[a]

compd		[M + 1]+	[M + 19]+	[M + 37]+	[M + 55]+
phenol		1.00	1.00		
methylphenol,	*o*-	1.00	0.50	0.06	
	m-	1.00	0.62	0.05	
	p-	1.00	0.85	0.30	
ethylphenol,	*o*-	1.00	0.40	0.06	
	m-	1.00	0.59	0.05	
	p-	1.00	0.78	0.20	
sec-butylphenol,	*o*-	1.00	0.15	0.05	
sec-amylphenol,	*p*-	1.00	0.30	0.14	
phenylphenol,	*o*-	1.00	0.063	0.13	
	p-	1.00	0.17	0.06	
dihydroxybenzene,	*o*-	1.00	0.18	0.16	0.03
	m-	1 00	0.58	0.06	0.01
	p-	1.00	0.95	0.53	0.04
chlorophenol,	*o*-	1.00	0.10		
	m-	1.00	0.77		
	p-	1.00	0.78		
aminophenol,	*o*-	1.00	0.42		
	m-	1.00	0.60		
	p-	1.00	0.64		
nitrophenol,	*o*-	0.41	1.00	0.11	
	m-	0.16	1.00	0.37	0.16
	p-	0.45	1.00	0.08	
hydroxybenzoic acid,	*o*-	0.75	1.00	0.06	
	m-	0.28	1.00	0.17	
	p-	0.41	1.00	0.06	
cyanophenol,	*p*-	0.26	1.00	0.07	

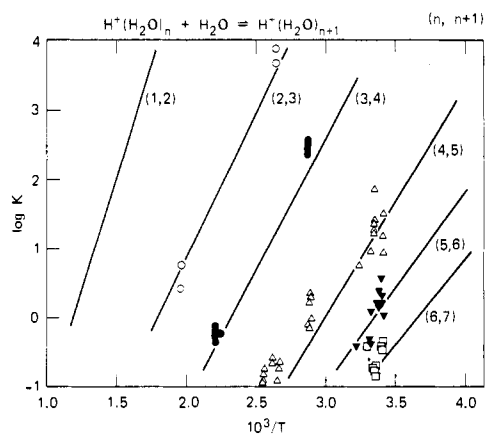[a] Obtained at 120 °C and 0.3 Torr H_2O.

vides an internal check on the quality of the data. Figure 6 compares our results for the various equilibria in water with those from Kebarle's laboratory (solid lines).[14,15] The quite good agreement between the two sets of data indicates that thermochemical equilibrium is, in fact, established under the conditions of our experiments.

Results

Conventional Source. Table I shows the water chemical ionization mass spectra of 27 substituted phenols introduced via the solids probe into a conventional chemical ionization source.[3,5,7] All of these compounds formed the MH^+ ions, as well as one or more hydrogen-bonded clusters $MH^+(H_2O)_n$. In no case was any fragmentation of MH^+ ion observed. Because the relative intensities of the various cluster ions are sensitive to both source temperature and pressure, every effort was made to keep these parameters constant. Although accurate measurements were not possible with this source, the nominal values were 120 °C and 0.3 Torr. Under these conditions, the spectrum of pure water contained ions up to m/e 91 corresponding to the species $H^+(H_2O)_n$ for $n = 1$-5. The relative intensities of the ions at m/e 19, 37, 55, 73, and 91 were (0.12):(0.14):(0.62):(1.00):(0.029), while the intensities expected[14,15] at equilibrium are (2.0×10^{-12});(1.2×10^{-3}):

(0.52):(1.00):(0.0080). Although the intensities of the two smallest clusters are much too large to have come from a population of ions at thermal equilibrium, the intensities of the other three are equivalent within experimental error to the equilibrium values (see below).

The relative intensities of the various $MH^+(H_2O)_n$ ions given in Table I are reproducible with care to within ±0 05. Thus it is possible on the basis of their water CI spectra alone to identify the ortho, meta, and para isomers of the methylphenols, the ethylphenols, the dihydroxybenzenes, and the hydroxybenzoic acids.

In order to determine the origins of these analytically useful effects, the mass spectrometer was modified as described above for pulsed high-pressure operation. The equilibrium constants and free-energy changes for reaction 8 for 17 substituted phenols are given in Table II. These values are averages of at
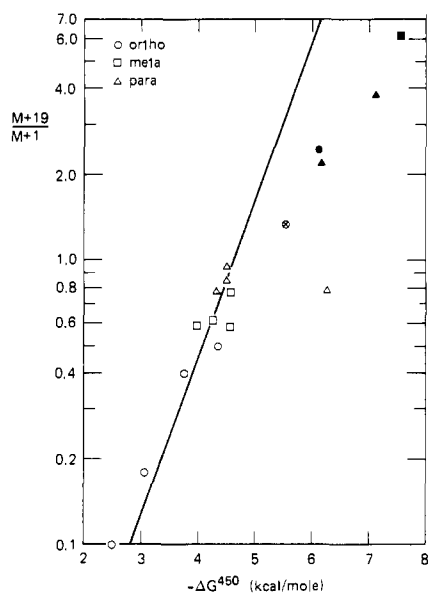
Figure 7. Correlation of the ratio of the $MH^+(H_2O)$ to MH^+ intensities from Table I with the measured value of ΔG^{450} for reaction 8 from Table II. The open symbols are compounds which protonate on the hydroxy group. The solid symbols are the nitrophenols. $\triangle$ p-cyanophenol; $\otimes$, o-hydroxybenzoic acid. The excellent correlation between the conventional water CI data and the equilibrium measurements shows that the sample ion concentrations are at or near equilibrium in the CI source. The solid line is the relationship calculated from the nominal conditions in the conventional CI source and the measured values of $-\Delta G^{450}$. See text.

Table II. Equilibrium Constants of the Substituted Phenols

compd		K, Torr^{-1a}	T, K	$-\Delta G$, kcal/mol^b	$-\Delta G^{450}$, kcal/mol^c
methylphenol,	o-	0.193	447	4.43	4.35
	m-	0.135	454	4.16	4.27
	p-	0.226	447	4.57	4.49
ethylphenol,	o-	0.74	455	3.64	3.77
	m-	0.100	453	3.90	3.98
	p-	0.134	455	4.18	4.31
nitrophenol,	o-	3.64	427	6.72	6.11
	m-	18.4	427	8.10	7.49
	p-	3.89	427	6.78	6.17
hydroxyphenol,	o-	0.034	454	2.93	3.04
	m-	0.188	454	4.47	4.57
	p-	0.170	454	4.38	4.49
chlorophenol,	o-	0.037	436	2.89	2.51
	m-	0.296	443	4.76	4.57
	p-	1.28	453	6.19	6.27
cyanophenol,	p-	12.3	426	7.74	7.10
hydroxybenzoic acid,	o-	0.587	452	5.48	5.53

^{a} Equilibrium constant for the reaction $[MH]^+ + H_2O \rightleftarrows [MH_3O]^+$. ^{b} Standard state = 1 atm. ^{c} The $-\Delta G$ value at 450 K is calculated from the ΔG value at the temperature in the second column. The value of ΔS determined by Hiraoka et al.[16] for the reaction of protonated dimethyl ether with water has been used in the correction: $\Delta S = -26.5$ eu.

least two or (usually) more determinations. The ΔG values were reproducible to ± 0.4 kcal/mol which corresponds to $\pm 60\%$ variation in the equilibrium constant measurements. This is a much larger variability than that predicted from the expected experimental errors, and we are continuing our efforts to determine its origins. The source block and mounting plate are separately heated, but neither is temperature regulated. Because of the requirement that both of these thermally coupled parts stabilize at exactly the same temperature, it was impractical to obtain data for all of the compounds at exactly the same temperature. The right-hand column in Table II shows the free-energy change for formation of the hydrogen bond between the protonated phenol and a single water molecule corrected to 450 K using for ΔS the value of -26.5 eu, the experimental value obtained by Kebarle[16] for the hydrogen bond between protonated dimethyl ether and water. Even if the actual ΔS values for the phenols differed by as much as ± 10 eu, the largest error introduced would be only ± 0.24 kcal/mol for the worst case (cyanophenol). In most cases, the error would be less than ± 0.1 kcal/mol.

Figure 7 shows the excellent correlation between the ratio of the (M + 19) to the (M + 1) peak in the conventional water CI spectrum and the value of ΔG^{450} for the formation of the hydrogen bond. The open symbols represent compounds (the alkylphenols, chlorophenols, and dihydroxybenzenes) which are known to protonate on the hydroxy group.[7] The solid symbols are the nitrophenols. The water CI spectra of the nitrophenols (Table I) are very similar to that reported earlier[7] for nitrobenzene; $[M + 19]^+$ is the base peak with significant amounts of $[M + 37]^+$ also present.

Discussion

The existence of the correlation shown in Figure 7 clearly shows that the chemically interesting and analytically useful differences in the water CI spectra of these phenols (Table I) arise from differences in the thermochemical properties of the hydrogen-bonded cluster ions rather than from differences in the kinetics of their formation.

The fact that the relative intensities of the $MH^+ \cdot H_2O$ and MH^+ ions in the conventional water CI spectrum of a compound are related in a simple way to the free energy of formation of the hydrogen bond has important implications. It provides a sound physical basis for understanding our earlier observations[3,17] that the pattern of the various $MH^+(H_2O)_n$ ions in water CI spectra depends on the functionality of the sample molecules M, and that the pattern is remarkably constant for large numbers of molecules with the same single functional group.[17] By far the largest component of the hydrogen bond energy is the electrostatic energy,[18] which in this case depends almost entirely on the chemical identity of the functional group which is protonated. In the absence of specific intramolecular interactions such as hydrogen bonds to ortho groups, both ΔH and ΔS should be approximately the same regardless of the presence or identity of remote substituents. Thus, ΔG_f for a gas-phase hydrogen bond between a protonated molecule and water will be determined primarily by the functional group protonated with relatively small shifts due to the charge stabilizing or destabilizing effects of remote substituents.

The expected values of the ratio of $(M + 19)^+$ to $(M + 1)^+$ obtained from the conventional water CI spectra (Table I) can be calculated from the values of ΔG^{450} for formation of the hydrogen bond (Table II). For reaction 8, the equilibrium constant is

$$K = \frac{[MH^+ \cdot H_2O]}{[MH^+][H_2O]}$$

and $\Delta G = \Delta H - T\Delta S = -RT \ln K$. Assuming that both ΔH and ΔS are independent of temperature and further assuming that ΔS is the same for all of these phenols (see above), we have

$$\Delta G^{393} = \Delta G^{450} + 57\Delta S$$
$$= -RT \ln [H_2O] + RT \ln \{[(M + 19)^+]/[(M + 1)^+]\}$$

This theoretical relationship is plotted in Figure 7 for $\Delta S = -26.5$ eu and $[H_2O] = 0.3$ Torr.[19] It is worth noting that the best fit through the open symbols corresponds to 405 K and 0.55 Torr water pressure in the conventional CI source. An error of 12 K in the temperature is not at all unusual for the simple, uncompensated, and uncalibrated temperature indi-

cator on the conventional CI instrument; the possibility that the actual pressure might have been as high as 0.55 Torr is somewhat disconcerting but cannot be ruled out. Taken together, the data in Figure 7 suggest that at low values of $-\Delta G$, the ratio of $(M + 19)^+$ to $(M + 1)^+$ is indeed the equilibrium value, but that for larger equilibrium constants the experimental ratio is too low. This situation is reasonable since the observed signals are effectively averaged over a range of ion lifetimes in the source. $(M + 1)^+$ ions formed near the source exit slit may not remain in the source long enough to become completely equilibrated. The contribution of these ions to the overall spectrum would cause the observed ratio of $(M + 19)^+$ to $(M + 1)^+$ to be too low. Thus, while there is a qualitative correlation between ΔG and the observed ratio, the quantitative relationship breaks down for $-\Delta G > 5$ kcal/mol.

It has been our observation that in the conventional CI source, the relative intensities of the $H^+(H_2O)_n$ ions in pure water are usually those predicted, assuming thermochemical equilibrium for $n = 3, 4$, and 5, even though the intensities for $n = 1$ and 2 are much too large. Apparently the H_3O^+ and $H_5O_2^+$ ions arise from ionization by scattered electrons very near the ion exit slit. This explanation is supported by the observation that these nonequilibrium ions are only seen during and a few microseconds after the electron beam pulse in the pulsed high-pressure source. Therefore, they are not formed by collisonal dissociation of equilibrium ions,[20] since that mechanism would lead to a constant ratio of equilibrium to nonequilibrium species. Since these ions do not remain in the conventional source long enough to even approach equilibrium (five to ten collisions), the probability that they have reacted with any sample molecule (present at the level of one part or less in 10^3 of the water) is very small. Thus the *sample ion* peaks in CI can have relative intensities determined by *equilibrium ion* concentrations in the source even though a major fraction of the reagent ions appearing in the spectrum do not reach thermochemical equilibrium before leaving the source.

The present results provide a detailed example of the use of gas-phase hydrogen bond strengths as probes of the structure of protonated molecules. Of the 12 molecules in which we know from previous work[7] that protonation occurs on the hydroxy group, 8 form hydrogen bonds with $\Delta G_f^{450} = -4.3 \pm 0.4$ kcal/mol. The only compound with an ortho substituent in this cluster (see Figure 7) is *o*-methylphenol, a compound for which no ortho effect would be expected. The point for *o*-ethylphenol is on the correlation line, but the value of $-\Delta G_f^{450}$ for its hydrogen bond is sufficiently far below that for *o*-methylphenol to suggest that there is some interaction between the ethyl group and the protonated hydroxy group which is reduced by the addition of the water molecule. Both the 1,2-dihydroxybenzene and *o*-chlorophenol show significantly weaker hydrogen bonding to water. This is readily understood if adding the water molecule requires the breaking of an intramolecular hydrogen bond between the protonated hydroxy group and the ortho substituent. Thus, in cases where the site of protonation of a molecule may be inferred from its structure or other data, hydrogen bond strengths can be used to detect the presence of

intramolecular interactions. These studies need not be limited to large changes such as those due to ortho effects. The relative cluster ion intensities, such as those in Table I, may be used directly, and they are to be preferred both because they can be more precisely measured and because they are much more readily obtainable. For example, the difference in the hydrogen bond strengths between water and protonated *m*- and *p*-methylphenol is calculated from the data in Table 1 to be 0.25 kcal/mol.

In cases where the site of protonation of a molecule is not known in advance, it can often be determined from its water CI spectrum. The solid symbols in Figure 7 represent the data for the nitrophenols. Since both the complete pattern of $MH^+(H_2O)_n$ ions for these compounds (Table I) closely resemble that for nitrobenzene[7] and the hydrogen bonds to a single water molecule are much stronger than those found for protonated hydroxy groups, the nitrophenols must protonate on the nitro group.[21]

References and Notes

(1) SRI International, 204-A, Menlo Park, Calif. 94025.
(2) F. H. Field, *MTP Int. Rev. Sci.: Phys. Chem., Ser. One*, **5** (1972); E. Munson in "Interactions between Ions and Molecules", P. Ausloos, Ed., Plenum Press, New York, N.Y., 1975.
(3) P. Price, D. P. Martinsen, R. A. Upham, H. S. Swofford, Jr., and S. E. Buttrill, Jr., *Anal. Chem.*, **47**, 190 (1975).
(4) S. E. Buttrill, Jr., W. L. Reynolds, and M. A. Knoll, *Inorg. Chem.*, **15**, 2323 (1976).
(5) I. C. Wang, H. S. Swofford, Jr., P. C. Price, D. P. Martinsen, and S. E. Buttrill, Jr., *Anal. Chem.*, **48**, 491 (1976).
(6) P. Price, H. S. Swofford, Jr., and S. E. Buttrill, Jr., *Anal. Chem.*, **48**, 494 (1976).
(7) D. P. Martinsen and S. E. Buttrill, Jr., *Org. Mass Spectrom.*, **11**, 762 (1976).
(8) P. Kebarle in "Modern Aspects of Electrochemistry", B. E. Conway and J. O. M. Bockris, Ed., Plenum Press, New York, N.Y., 1974, Chapter 1.
(9) P. Kebarle in "Ion-Molecule Reactions", J. L. Franklin, Ed., Plenum Press, New York, N.Y., 1972, Chapter 7.
(10) Corning Glass Works, Corning Glass Works, Corning, N.Y.
(11) (a) L. N. Gall', R. N. Gall', and M. S. Stepanova, *Sov. Phys.-Tech. Phys.*, **13**, 790 (1968); (b) L. N. Gall', R. N. Gall', V. A. Demidova, and M. S. Stepanova, *ibid.*, **13**, 794 (1968); (c) N. K. Vasil'eva, L. N. Gall', E. M. Kleshow, E. B. Petrova, M. S. Stepanove, and G. V. Fridlyanskii, *Instrum. Exp. Tech. (Engl. Transl.)*, 665 (1968).
(12) A. Septier, "Focusing of Charged Particles", Vol. 1, Academic Press, New York, N.Y., 1967.
(13) C. F. Giese, *Rev. Sci. Instrum.*, **30**, 260 (1959); C. S. Lu and H. E. Carr, *ibid.*, **33**, 823 (1962).
(14) A. J. Cunningham, J. D. Payzant, and P. Kebarle, *J. Am. Chem. Soc.*, **94**, 7627 (1972).
(15) P. Kebarle, S. K. Searles, A. Zolla, J. Scarborough, and M. Arshadi, *J. Am. Chem. Soc.*, **89**, 6393 (1967).
(16) K. Hiraoka, E. P. Grimsrud, and P. Kebarle, *J. Am. Chem. Soc.*, **96**, 3359 (1974).
(17) S. E. Buttrill, Jr., presented at the 23rd Annual Conference on Mass Spectrometry and Allied Topics, Houston, Texas, May 25–30, 1975, Paper No. W-7.
(18) P. Kollman, *J. Am. Chem. Soc.*, **99**, 4875 (1977).
(19) We are indebted to a referee for suggesting this interpretation of the data.
(20) K. Hiraoka and P. Kebarle, *J. Am. Chem. Soc.*, **97**, 4179 (1975).
(21) This conclusion is supported by the CID–MIKE spectrum of *p*-nitrophenol. T. L. Kruger, R. Flammang, J. F. Litton, and R. G. Cooks, *Tetrahedron Lett.*, 4555 (1976).